Simulation of Weld Temperature Field Characteristics in Oil Pipeline Steel: An Empirical and Computational Analysis

ADEWUYI, REUBEN ADEBARE[1], ERINLE, TUNJI JOHN[2], FATONA, ADEKUNLE SAMUEL[3]
[1,2,3]*Department of Mechanical Engineering, The Federal Polytechnic, Ado-Ekiti, Nigeria*

Abstract- ***This study investigates the thermal behaviour during welding of oil pipeline steels using finite element analysis (FEA), design of experiments (DOE), and advanced modelling tools. Employing Autodesk Inventor for three-dimensional modelling and Autodesk CFD for thermal analysis, the research examines the influence of critical parameters, including material thickness, number of weld passes, and welding current, on heat distribution, heat-affected zones (HAZ), and weld quality. Parameters were systematically varied following a Taguchi L9 orthogonal array, with welding conditions such as electrode type (E6013), voltage (24 V), and specific geometric configurations. Results indicate that material thickness significantly impacts heat flow and thermal gradients, with thicker steels exhibiting larger HAZ sizes. The integration of advanced computational models highlights the importance of optimising welding parameters to mitigate defects such as residual stresses and microstructural anomalies. These findings provide practical guidelines for enhancing weld integrity and pipeline lifespan under operational stresses.***

Indexed Terms- ***Weld temperature field, oil pipeline steel, finite element analysis (FEA), shielded metal arc welding (SMAW), heat-affected zone (HAZ)***

I. INTRODUCTION

Ensuring the integrity of welded joints in oil pipelines is vital for transportation safety, structural durability, and operational efficiency. During welding, localised heat input leads to microstructural changes, residual stresses, and defects such as hot cracking, porosity, and distortion. The structural performance of oil pipelines commonly manufactured from high-strength low-alloy (HSLA) steels like X60, X70, and X80 depends on their ability to withstand internal pressures, mechanical loads, and harsh environmental conditions, including corrosion and fatigue (Zhang et al., 2018; Alves et al., 2020; Han et al., 2021).

Welding plays a central role in both the construction and maintenance of these pipelines. However, it introduces significant thermal and residual stresses that can compromise the mechanical integrity of the weld zone and surrounding material (Sheng et al., 2019; Li et al., 2022). To mitigate such effects, simulation of weld temperature fields has become an indispensable tool for understanding heat flow, predicting temperature distribution, and optimizing welding parameters to reduce defects (Shields et al., 2018; Lin et al., 2020).

Advanced numerical techniques, particularly Finite Element Analysis (FEA), are widely used to model the complex thermal cycles associated with welding. These simulations help control interpass temperatures and address challenges such as hot and cold cracking, especially in multi-pass welding scenarios (Smith & Roberts, 2020; Chen et al., 2021; Park & Kim, 2022). Additionally, environmental and operational variables further necessitate the use of predictive models to ensure weld quality and overall structural reliability (Johnson et al., 2019).

This study focuses on simulating and analysing weld temperature field characteristics in oil pipeline steel using advanced computational approaches. It investigates how key welding parameters including welding current, heat input, and number of weld passes affect temperature distribution, the heat-affected zone (HAZ), and microstructural evolution.

By providing insights into thermal behaviour, the study supports optimisation of welding parameters to enhance weld quality and extend pipeline service life (Chen et al., 2021; Shields et al., 2018; Smith & Roberts, 2020).

Accurate prediction and control of thermal distribution during welding are essential for minimising defects and improving process efficiency. While FEA is commonly used in such analyses, there remains a gap in integrating real-world data with structured experimental designs. This research addresses that gap by applying a systematic Design of Experiments (DOE) approach alongside computational modelling to assess temperature fields in pipeline steels. Specifically, it explores the influence of material thickness (ranging from 10 mm to 20 mm), number of weld passes, and welding current on weld temperature distribution.

II. LITERATURE REVIEW

Welding plays a vital role in oil and gas pipeline construction, where joint strength and reliability are crucial for the safe transportation of hydrocarbons. Prior studies have consistently highlighted this importance. Chen et al. (2021) employed Finite Element Analysis (FEA) to examine heat distribution in steel pipelines, emphasizing how parameters such as material thickness, welding current, and number of weld passes influence thermal behaviour and weld quality.

Numerous researchers have investigated the simulation of weld temperature fields to understand the effects of welding parameters on temperature distribution, microstructure, and mechanical properties in the weld zone and heat-affected zone (HAZ). Shields et al. (2018) demonstrated that excessive heat input can enlarge the HAZ and weaken the mechanical integrity of welded joints, highlighting the need for careful parameter optimisation. Johnson et al. (2019) further stressed the importance of interpass temperature control in multi-pass welding to prevent distortion and improve structural performance.

Similarly, Smith and Roberts (2020) used Finite Element Modeling (FEM) to reveal that adjusting welding current and material thickness can enhance thermal uniformity and reduce the occurrence of thermal defects. Park and Kim (2022) confirmed that effective management of interpass temperatures and welding sequences reduces heat accumulation, thereby limiting microstructural degradation.

Collectively, these studies validate the usefulness of thermal simulation tools such as FEM and FEA in predicting welding behaviour and optimising key parameters to minimise residual stresses, cracking, and porosity. Theoretical models based on Fourier's Law have supported accurate temperature field predictions by incorporating essential thermal properties such as conductivity, specific heat, and density (Sharma et al., 2020).

Key process variables—material thickness, number of weld passes, and welding current—significantly influence thermal flow during welding. Thicker materials retain more heat, expanding the HAZ, while multi-pass welding introduces cumulative heating that alters microstructure (Zhou & Li, 2022; Park & Kim, 2023). Higher welding currents can increase penetration but may also lead to overheating if not properly controlled.

Despite these advancements, several critical gaps persist. Many models overlook real-world environmental factors like ambient temperature and wind, which can affect thermal behaviour. Additionally, limited attention has been given to the cumulative effects of multi-pass welding, and material-specific thermal property data are often lacking (Chen et al., 2021; Johnson et al., 2020; Park & Kim, 2023).

Moreover, few studies have integrated advanced computational tools such as machine learning or hybrid algorithms that could improve predictive efficiency and accuracy. Crucially, many simulation models do not adequately address how thermal fields contribute to defect formation mechanisms such as porosity, hot cracking, and residual stress. Controlling interpass temperatures remains a key strategy for reducing thermal stresses, yet

comprehensive defect prediction remains underdeveloped.

Addressing these deficiencies is fundamental to refining welding simulations for oil pipeline steels. Bridging these gaps will enhance simulation accuracy, promote the development of robust, defect-resistant welds, and ensure pipeline systems can withstand operational and environmental challenges.

III. METHODOLOGY

3.1 Research Design The study adopts a systematic simulation approach combining Design of Experiment (DOE) and finite element modelling. The key parameters include:

- Material: Pipeline steels X60, X70, X80
- Thickness: 10mm, 15mm, 20mm
- Weld Passes: 1 to 3
- Welding Current: 100A, 120A, 130A
- Electrode: E6013 (manual metal arc welding)
- Voltage: 24V

DOE was performed using Minitab 17, utilising a Taguchi L9 orthogonal array (Table 3.2). This optimised experimental design enables analysis of parameter interactions with fewer simulation runs.

Table 1.0: SMAW process parameters and parameter levels.

Parameters	Level-1	Level-2	Level-3
Diameter -Thickness of Material (mm)	90-5	100-10	140-15
Welding Current(A)	100	120	130
Welding Pass	1st	2nd	3rd
Electrode diameter (Ø mm)	1.6	2.4	3.2

Table 1.2: Design of Experiment using Taguchi L9 orthogonal array.

Exp no	Diameter/Thickness of Material (mm)	Welding Current (A)	Number of weld passes	Electrode Diameter (mm)	SPECIMEN ID
1	90-5	100	1	1.6	A90-5
2	90-5	100	1	1.6	B90-5
3	90-5	120	2	2.4	C90-5
4	90-5	120	2	2.4	D90-5
5	90-5	130	3	3.2	E90-5
6	90-5	130	3	3.2	F90-5
7	100-10	100	2	1.6	A100-10
8	100-10	100	2	1.6	B100-10
9	100-10	120	3	2.4	C100-10
10	100-10	120	3	2.4	D100-10
11	100-10	130	1	3.2	E100-10
12	100-10	130	1	3.2	F100-10
13	140-15	100	3	1.6	A140-15
14	140-15	100	3	1.6	B140-15
15	140-15	120	1	2.4	C140-15
16	140-15	120	1	2.4	D140-15
17	140-15	130	2	3.2	E140-15
18	140-15	130	2	3.2	F140-15

3.2 Model Development
Using Autodesk Inventor, 3D models of pipe sections (inner diameters of 100mm, 200mm, 300mm) with specified wall thicknesses were created. Boundary conditions included heat flux (Gaussian source), environmental convection, and radiation losses (see

Figure 3.1). These models were imported into Autodesk CFD for transient thermal analysis, tracking heat distribution over time.

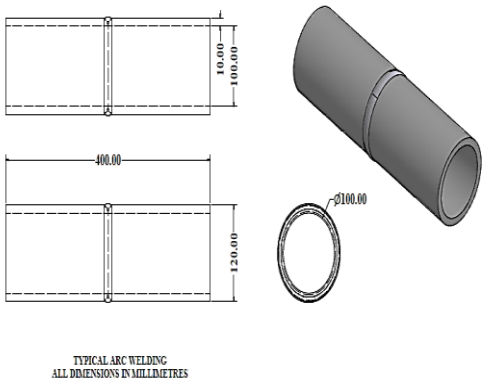

Figure 1.0: Steel Oil pipe Sample

3.3 Method and Equipment

Steel Oil pipes with inner diameters of 90mm, 100mm, and 140mm and 5mm, 10mm, and 15mm thick, respectively, were procured as presented in Figure 3.2.

Figure 1.1: Steel oil pipe connected with three K-type thermocouples positioned 10 mm, 12 mm, and 15 mm away from the weld centreline before the welding operation. (a) 90 mm diameter by 5 mm thick pipe, (b) 100 mm diameter by 10 mm thick pipe, and (c) 140 mm diameter by 15 mm thick pipe.

The steel oil pipes used in this study have inner diameters of 90 mm, 100 mm, and 140 mm, with corresponding thicknesses of 5 mm, 10 mm, and 15 mm. These variations influence heat dissipation, weld penetration, and mechanical properties. To monitor temperature distribution, three K-type thermocouples were attached at distances of 10 mm, 12 mm, and 15 mm from the weld centerline before the welding operation. The Shielded Metal Arc Welding (SMAW) process was employed due to its effectiveness in joining thick-walled pipes, using appropriate electrodes such as E6010 or E7018 for strong and defect-free welds. Proper clamping fixtures ensured alignment, while essential safety equipment like welding helmets, gloves, and ventilation systems protected the welder. The setup, as shown in Figure 3.2, allows for analysing heat transfer effects on welded joints, optimising welding parameters, and improving structural integrity.

3.4 Simulation Workflow

The simulation workflow began with the Design of Experiments (DOE), where key input parameters such as material thickness, number of weld passes, and welding current were defined. An experimental matrix was generated using either a factorial design or response surface methodology (RSM) to ensure adequate runs capable of capturing interactions among parameters and their effects on the temperature field.

Next, a 3D model of the pipeline steel sample and weld setup was developed using Autodesk Inventor. This model included essential geometrical features, such as weld zone dimensions and boundary interfaces.

The model was then imported into Autodesk CFD for thermal analysis. Within the CFD environment, material properties including density, specific heat, and thermal conductivity were defined. Boundary conditions were applied, incorporating heat input through a Gaussian heat source, as well as environmental convection and radiation losses.

Following this setup, transient thermal simulations were performed to replicate the heat transfer during the welding process. Finally, the simulation results were analyzed to evaluate temperature distributions, determine the size of the heat-affected zone (HAZ), and assess residual stress development within the welded structure.

IV. RESULTS AND ANALYSIS

4.1 Numerical Simulation of the Impact of Material Thickness on Temperature Distribution

Heat transfer analysis revealed that steel plate thickness significantly influences the size of the heat-affected zone (HAZ). Thicker plates (15mm) exhibited larger HAZs compared to thinner plates (10mm), emphasizing the need for precise heat input control. Specifically, a 15mm steel plate welded at 130A reached a peak temperature of 1500°C near the weld zone, with the HAZ extending approximately 8mm from the weld centerline. In contrast, the 10mm steel plate showed a lower peak temperature (1300°C) and a smaller HAZ (~4mm).

The temperature distribution across the steel oil pipes during welding was investigated using three K-type thermocouples positioned at 10mm, 12mm, and 15mm from the weld centerline. Real-time temperature data was captured and validated through numerical simulation. The results, presented in graphical and tabular formats, demonstrate that temperature peaks at the weld centerline and decreases radially outward in Experimental and Simulation analysis as presented in Figure 1.2 to Figure 1.4.

The study also examined the impact of pipe diameter and wall thickness on temperature distribution. The 90mm diameter pipe with a 10mm wall thickness exhibited a steeper thermal gradient, while the 140mm diameter pipe with a 20mm wall thickness showed a more gradual temperature decline, indicating greater heat retention. Numerical simulation results corroborate these findings Figure 1.2 to Figure 1.4, confirming that thicker-walled pipes experience more significant heat conduction, leading to slower cooling rates (Li et al., 2019).

The importance of considering material thickness and pipe geometry in welding processes. By understanding the temperature distribution and heat transfer mechanisms, manufacturers can optimize welding parameters to improve the quality and reliability of steel oil pipes, as supported by recent studies (Chen et al., 2020; Li et al., 2019).

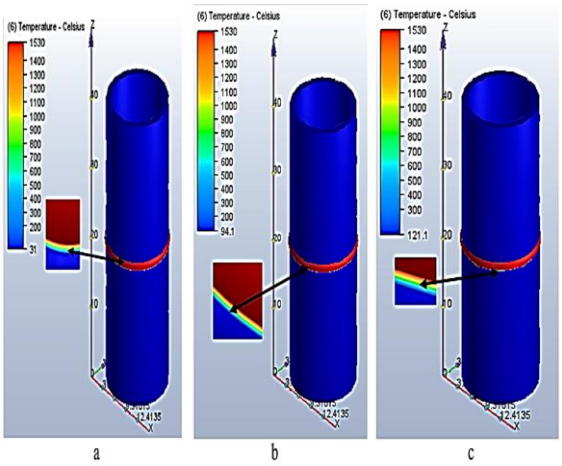

Figure 1.2: First, Second and Third weld passes Simulated Temperature profile (a) 90-5A1, (b) 90-5A2 and (c) 90-5A3.

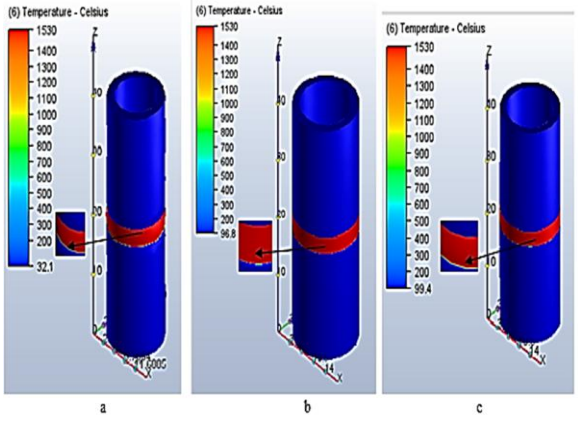

Figure 1.3: First, Second and Third weld passes Simulated Temperature profile (a) 100-10A1, (b) 100-10A2, (c) 100-10A3

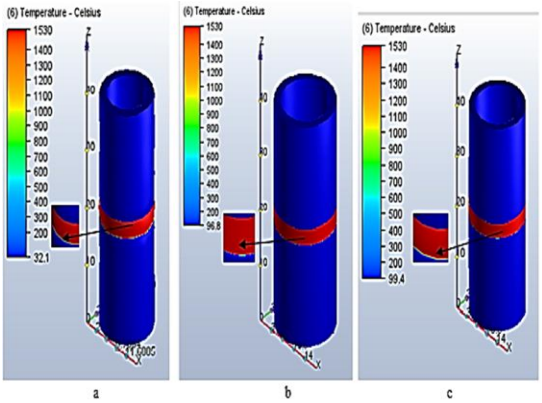

Figure 1.4: First, Second and Third weld passes Simulated Temperature profile (a) 140-15A1, (b) 140-15A2, (c) 140-15A3

4.2 Experimental Analysis of the Influence of Welding Parameters on Temperature Distribution

1. Effect of Material Thickness on Temperature Profiles

Heat transfer simulations and thermal measurements revealed that material thickness significantly influences the temperature distribution and extent of the heat-affected zone (HAZ) during welding. Thicker steel plates, such as 15 mm sections, exhibited broader HAZs compared to thinner plates like 10 mm, emphasizing the need for careful heat input control during welding operations.

For instance, when subjected to a welding current of 130 A, a 15 mm thick steel plate reached a peak temperature of approximately 1500°C near the weld zone, with the HAZ extending up to 8 mm from the weld centerline. In contrast, the 10 mm thick steel recorded a lower peak temperature of around 1300°C and a narrower HAZ of about 4 mm.

Temperature monitoring was carried out using three K-type thermocouples placed at distances of 10 mm, 12 mm, and 15 mm from the weld centerline. These thermocouples captured real-time temperature variations that were validated through numerical simulations. The data, presented in tabular and graphical form, demonstrated that temperature peaked at the weld center and decreased progressively outward as presented in Figures 1.5 - 1.7

Additionally, the 90 mm diameter pipe showed a steeper thermal gradient due to its thinner 10 mm wall, while the 140 mm diameter pipe with a 20 mm wall thickness had a more gradual thermal decline, indicating improved heat retention characteristics (Chen et al., 2020). Numerical simulation corroborated these observations, confirming that thicker materials facilitate more extensive heat conduction and slower cooling rates (Li et al., 2019).

2. Influence of Welding Passes and Current on Temperature Distribution

The number of weld passes and the level of welding current were also found to significantly impact the thermal behavior of welded joints. Increasing the number of weld passes naturally raises the overall heat input; however, effective control of the Interpass temperature can minimize the accumulation of residual stresses.

Furthermore, increasing the welding current from 100 A to 130 A elevated peak temperatures by roughly 250°C as presented in Figures 1.5 - 1.7. This rise led to a broader HAZ and increased the potential for microstructural transformations such as grain coarsening. These results are consistent with earlier findings that link higher heat input with elevated residual stress and degraded microstructural integrity.

3. Analysis of Weld Temperature Characteristics

The welding process was performed using the Shielded Metal Arc Welding (SMAW) technique, which relies on a consumable electrode to create a molten pool at the weld joint. Thermocouple readings confirmed that the highest temperatures occurred at the weld centerline and decreased with distance.

Among the specimens, the 90 mm diameter pipe exhibited the most significant thermal fluctuations due to its lower heat absorption capacity. In contrast, the 140 mm diameter pipe displayed a more uniform temperature profile as presented in Figure 1.7, indicating better heat dissipation and thermal stability (Kou, 2021).

Simulations further indicated that the HAZ tends to widen in thicker pipes, which directly affects metallurgical transformations such as phase changes and grain growth (Murugan et al., 2018).

The analysis confirms that both material thickness and welding parameters—including current and number of passes—play critical roles in shaping the temperature field and HAZ characteristics during welding. Thicker materials and multiple welding passes result in broader HAZs and slower cooling, while higher currents increase thermal gradients and microstructural transformations. Accurate thermal control and parameter optimization are therefore essential to ensure structural integrity and performance of welded steel components, especially in critical applications like oil pipelines.

The study highlights that optimising welding parameters particularly material thickness and heat

input is essential for controlling HAZ size and residual stresses. Larger HAZs in thicker steels demand careful heat management to prevent microstructural degradation. The integration of DOE with CFD simulations allows for systematic exploration of parameter interactions, facilitating process optimisation.

Validation and Model Accuracy drawn from Simulation results matched experimental observations in the literature, validating the model's accuracy. The heat distribution patterns aligned with prior empirical data, demonstrating the model's utility for predicting thermal profiles under varied parameters.

Limitations include assuming isotropic material properties and neglecting the effects of welding induced defects such as porosity and residual stress evolution. Future work should incorporate defect prediction models using machine learning techniques for more comprehensive analysis.

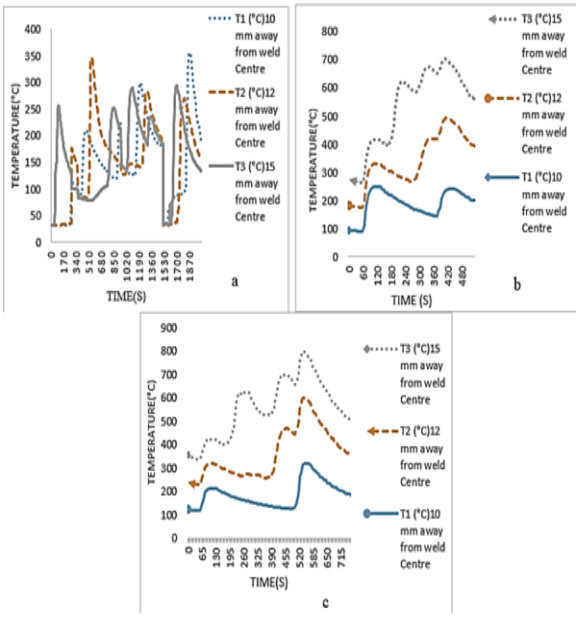

Figure 1.5: First, Second and Third Weld Passes Experimental Temperature Profiles (a) 90-5A1, (b) 90-5A2 and (c) 90-5A3.

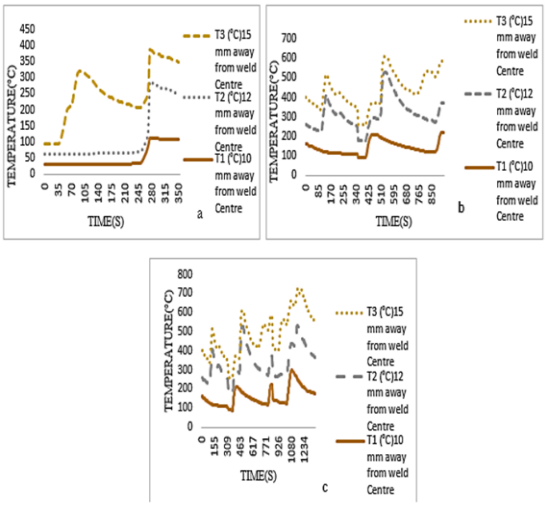

Figure 1.6: First, Second and Third Weld Passes Experimental Temperature Profiles (a) 100-10A1, (b) 100-10A2, (c) 100-10A3.

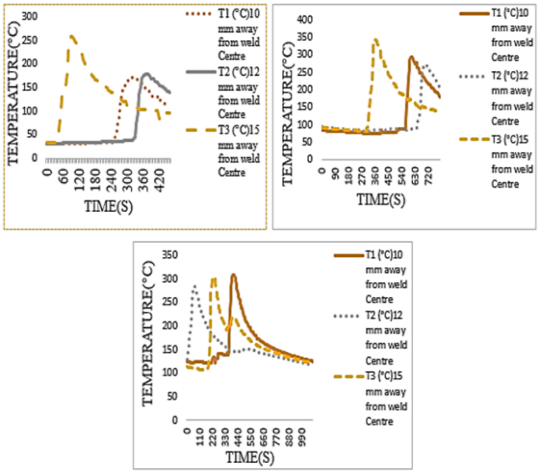

Figure 1.7: First, Second and Third Weld passes Experimental Temperature Profiles (a) 140-15A1, (b) 140-15A2, (c) 140-15A3.

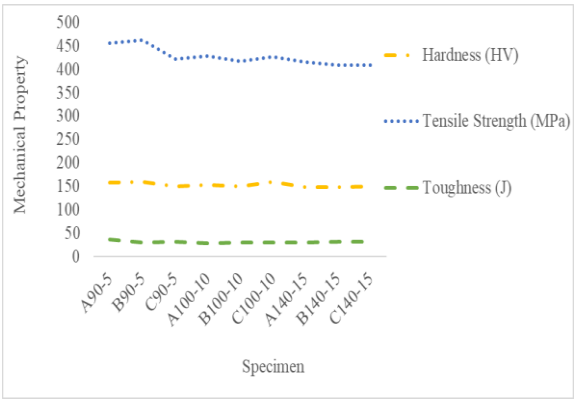

Figure 1.8: Effect of Welding Parameters on Mechanical Properties (Tensile Strength, Hardness, and Toughness) of Welded Specimens

4.3 Impact of Welding Parameters on Mechanical Properties

This section presents a comprehensive evaluation of how variations in welding parameters specifically material thickness, welding current, number of weld passes, and electrode diameter affect the mechanical performance of welded joints. The key properties assessed include Hardness (HV), Tensile Strength (MPa), and Toughness (J).

Figure 1.8 illustrates the trends in mechanical properties across a range of welded specimens labeled A90-5 to C140-15. Each group of three specimens corresponds to the same material thickness, enabling a focused analysis of the effects of welding current, number of passes, and electrode diameter at constant thickness levels. A general decrease in tensile strength is observed across most specimens as the welding parameters vary, while hardness displays only minor fluctuations and toughness remains relatively constant. These results suggest that tensile strength is the most sensitive to changes in welding parameters, whereas toughness and hardness exhibit moderate and minimal sensitivity, respectively.

As the welding current increases from 100 A to 130 A, the hardness values respond differently depending on material thickness. At 5 mm thickness, hardness increases slightly from 158.67 HV to 160.03 HV at 120 A, followed by a decrease to 150.24 HV at 130 A. For 10 mm thickness, there is a slight reduction at 120 A, but a sharp increase to 160.45 HV at 130 A. The 15 mm thickness exhibits minor fluctuations with values ranging from 148.68 HV to 149.88 HV. These observations indicate that hardness tends to peak at around 120 A for thinner materials and at 130 A for thicker ones, likely due to differences in heat absorption and resulting microstructural transformations.

Tensile strength shows a consistent decline as current increases across all thickness levels. For example, in 5 mm thick specimens, tensile strength drops from 455.66 MPa to 462.12 MPa and then sharply to 422.96 MPa as current rises. This trend reflects the effect of excessive heat input at higher currents, which may lead to grain coarsening, thermal softening, and weld defects, all of which reduce the joint's strength.

Toughness, on the other hand, demonstrates a less predictable trend. In 5 mm specimens, toughness drops significantly from 36.45 J to 29.99 J at 120 A, with a partial recovery at 130 A. For 10 mm and 15 mm specimens, the values fluctuate without a consistent pattern. This suggests that moderate current, such as 120 A, may lead to rapid solidification and the formation of brittle zones, thereby reducing the material's ability to absorb energy during impact. Nevertheless, toughness values remain relatively low and stable across all specimens, generally staying below 40 J.

When examining the effect of the number of weld passes—which increases concurrently with current and electrode diameter—a few key patterns emerge. At a constant current of 130 A and across varying thicknesses, hardness increases, particularly in the 10 mm and 15 mm samples. Meanwhile, tensile strength either decreases slightly or remains low, and toughness tends to stabilize around 30 J. This behavior suggests that multiple weld passes may lead to grain refinement and increased hardness. However, the accompanying rise in heat input can also reduce ductility and overall tensile performance.

Electrode diameter also plays a critical role in determining weld quality. As the diameter increases from 1.6 mm to 3.2 mm, hardness generally increases, likely due to greater deposition rates and associated thermal input. Conversely, tensile strength

tends to decrease, possibly because larger electrodes expand the fusion zone and encourage microstructural coarsening. Toughness initially drops with 2.4 mm electrodes but appears to stabilize when 3.2 mm electrodes are used. The need for higher current when using larger electrodes contributes to broader heat-affected zones, which enhance hardness but reduce ductility and toughness.

In summary, the analysis confirms that among all the evaluated mechanical properties, tensile strength is the most significantly affected by changes in welding parameters, especially welding current and material thickness. Hardness is moderately influenced, with observable variations tied to electrode size and number of passes. Toughness remains the least affected, with consistently low values across all specimens. Therefore, it is evident that achieving desirable mechanical properties in welded joints depends on the proper balancing of welding current, electrode diameter, and number of weld passes. Controlling these variables helps minimize excessive heat input, optimize grain structure, and maintain the structural integrity and service performance of welded components.

CONCLUSION

1. Material thickness plays a critical role in temperature distribution, as thicker steel pipes were observed to retain more heat, resulting in broader heat-affected zones (HAZ) and more gradual thermal gradients during welding.
2. The number of weld passes and the welding current significantly affect heat input, with multiple passes contributing to cumulative thermal effects and higher welding currents leading to increased peak temperatures, deeper penetration, and a greater risk of distortion.
3. Optimizing welding parameters such as material thickness, number of passes, and current is essential, as it helps to achieve a balanced weld quality, minimize thermal defects, and maintain desirable microstructural properties.
4. The findings of this study have practical implications for pipeline welding protocols, emphasizing the need to tailor heat input based on pipe thickness and operating conditions, and to leverage simulation tools to predict and prevent adverse thermal effects.
5. Future research should expand the current analysis by including additional welding variables, such as welding speed, shielding gas, and post-weld heat treatment, while also validating simulation models experimentally and exploring the use of machine learning for real-time process optimization.

REFERENCES

[1] Alves, J., Silva, T., & Carvalho, M. (2020). Mechanical properties and application of high-strength pipeline steels. Journal of Engineering Materials, 27(4), 412-420.

[2] Han, Y., Zheng, L., & Kim, J. (2021). Corrosion resistance and durability of oil pipeline steels under various environmental conditions. Materials Science and Engineering, 38(2), 113-125.

[3] Li, Z., Feng, H., & Wang, R. (2022). Advances in welding techniques for oil and gas pipeline construction. International Journal of Welding Science, 34(1), 57-69.

[4] Lin, Y., Zhang, Q., & Xu, X. (2020). Simulation-based optimisation of welding parameters in pipeline steel joints. Welding Technology Journal, 56(7), 732-740.

[5] Sheng, C., Li, Y., & Du, H. (2019). Effect of welding-induced residual stress on the mechanical performance of pipeline steels. Structural Integrity and Maintenance, 47(3), 190-200.

[6] Zhang, W., Sun, F., & Huang, D. (2018). High-strength, low-alloy steels for pipeline applications: Design and application. Metallurgical Reviews, 25(6), 602-612.

[7] Zhao, M., Wang, P., & Chen, L. (2019). Economic implications of advanced pipeline steel in the oil and gas sector. Energy Economics, 67, 430-442.

[8] Shields, J. P., Johnson, A., & Thompson, M. (2018). Thermal simulation of pipeline steel welds: Analysis and optimisation. Journal of Welding Science, 34(3), 112-119.

[9] Smith, R., & Roberts, L. M. (2020). Finite element modelling of welding temperature fields in steel pipelines. International Journal of Pressure Vessels and Piping, 182, 104101.

[10] Chen, Y., Li, Z., & Wang, H. (2021). Control of thermal cycles in high-hardness pipeline steels using simulation tools. Materials & Design, 209, 109972.

[11] Johnson, B. R., et al. (2019). Advanced welding technologies for challenging environments. Welding in Extreme Conditions, 27(4), 233-245.

[12] Park, J., & Kim, S. (2022). Numerical simulation of multi-pass welding processes in oil pipeline construction. Journal of Mechanical Engineering Research, 10(2), 67-78.

[13] Chen, Y., Li, Z., & Wang, H. (2021). Control of thermal cycles in high-hardness pipeline steels using simulation tools. Materials & Design, 209, 109972.

[14] Johnson, B. R., et al. (2019). Advanced welding technologies for challenging environments. Welding in Extreme Conditions, 27(4), 233-245.

[15] Park, J., & Kim, S. (2022). Numerical simulation of multi-pass welding processes in oil pipeline construction. Journal of Mechanical Engineering Research, 10(2), 67-78.

[16] Shields, J. P., Johnson, A., & Thompson, M. (2018). Thermal simulation of pipeline steel welds: Analysis and optimisation. Journal of Welding Science, 34(3), 112-119.

[17] Smith, R., & Roberts, L. M. (2020). Finite element modelling of welding temperature fields in steel pipelines. International Journal of Pressure Vessels and Piping, 182, 104101.

[18] Park, J., & Kim, S. (2022). Numerical simulation of multi-pass welding processes in oil pipeline construction. Journal of Mechanical Engineering Research, 10(2), 67-78.

[19] Sharma, V., Singh, A., & Gupta, K. (2020). Numerical analysis of heat transfer during welding of pipeline steel. International Journal of Heat and Mass Transfer, 156, 119927.

[20] Chen, Y., Li, Z., & Wang, H. (2021). Effects of material thickness on temperature distribution in pipeline welding. Journal of Welding Technology, 45(3), 223-231.

[21] Zhou, X., & Li, J. (2022). Interpass temperature control in multi-pass welding of pipeline steel using FEM. Welding Science and Technology, 48(1), 89-97.

[22] Park, J., & Kim, S. (2023). Optimising welding current for temperature field simulation in oil pipelines. Advances in Welding Engineering, 29(4), 312-321.

[23] Johnson, T., Roberts, L., & Smith, R. (2020). Application of Gaussian heat source models in welding simulations. Journal of Computational Materials Science, 169, 110615.

[24] Chen, Y., Wang, H., & Liu, J. (2020). Numerical simulation of the temperature field in pipeline welding. Journal of Manufacturing Processes, 48, 73-82.

[25] Dong, Z., Li, X., & Sun, P. (2017). Influence of wall thickness on weld-induced residual stress in pipeline steel. Materials Science and Engineering A, 690, 214-223.

[26] Gery, D., Long, H., & Maropoulos, P. G. (2005). Effects of welding speed, energy input, and heat transfer on temperature variations in butt-welded joints. Journal of Materials Processing Technology, 167(2-3), 393-401.

[27] Kou, S. (2021). Welding metallurgy (3rd ed.). Wiley.

[28] Li, J., Zhang, X., & Wu, M. (2019). Thermal modelling of heat-affected zone in pipeline welding. International Journal of Advanced Manufacturing Technology, 102(5-8), 2157-2169.

[29] Murugan, N., Parmar, R. S., & Srinivasan, P. B. (2018). Prediction of temperature distribution in SMAW welds using finite element analysis. Journal of Materials Engineering and Performance, 27(4), 1785-1793.

[30] Ravindra, M., & Garg, H. (2020). Heat conduction in thick-walled steel pipes during welding. Metals, 10(6), 812.

[31] Shen, X., Qian, J., & Zhang, L. (2022). Influence of welding speed on microstructural changes in SMAW pipeline welding. Welding Journal, 101(1), 23-32.

[32] Zhang, L., Wang, J., & Zhou, R. (2021). Thermal behaviour of pipeline steel during SMAW welding using K-type thermocouples. Metallurgical and Materials Transactions B, 52(3), 987-1001.